

Interstitial-oxygen-atom diffusion in MgO

T. Brudevoll

Institute of Physics and Astronomy, Aarhus University, DK-8000 Aarhus C, Denmark

E. A. Kotomin

*Institute of Physics and Astronomy, Aarhus University, DK-8000 Aarhus C, Denmark
and Institute of Solid State Physics, University of Latvia, 8 Kengaraga Street, Riga LV-1063, Latvia*

N. E. Christensen

Institute of Physics and Astronomy, Aarhus University, DK-8000 Aarhus C, Denmark

(Received 17 August 1995)

The atomic and electronic structure of the radiation-induced Frenkel defects O_i^0 in MgO crystals is calculated. A full-potential linear-muffin-tin-orbital method combined with a 16-atom supercell is used for the optimization of the interstitial defect geometry. It is found that energetically the most favorable ground state O_i configuration is the (111) dumbbell centered at a regular oxygen site, whereas face-centered and cube-centered configurations are higher in energy by 1.45 eV and 3.57 eV, respectively. The (111) configuration is close in energy to the (110) configuration, which allows the dumbbell to rotate easily on a lattice site. In all these four cases the interstitial oxygen atom attracts considerable additional electron density from its nearest regular O^{2-} ions, which makes it close to the O_i^- ion rather than a neutral atom. The mechanism and the relevant activation energy for O_i diffusion are discussed in the light of available experimental data.

I. INTRODUCTION

Ceramics based on the MgO- Al_2O_3 system are known as prospective materials for fusion reactors, for which purpose they have to maintain structural and electric integrity under irradiation with fast neutrons, γ rays, and high energy particles.¹ Such an irradiation produces a number of Frenkel defects, i.e., interstitial atoms and vacancies. Secondary diffusion-controlled reactions between these primary radiation defects can result in the appearance of defect clusters, dislocation loops, and voids affecting considerably the mechanical properties of the ceramics. This was a main motivation for the intensive study in recent years on the mechanism and kinetics of radiation damage in oxide materials, in particular, MgO and Al_2O_3 .^{2,3} Several kinds of radiation-induced point defects have been investigated, the simplest ones are called F^+ and F centers (O vacancy trapped one and two electrons, respectively).⁴ However, surprisingly little is known so far about their counterparts, interstitial oxygen atoms, O_i . In alkali halides (e.g., KCl, KBr) with fcc crystal structure and high ionicity like MgO, such radiation-induced interstitial halide atoms, X_i^0 , are very well studied, both experimentally and theoretically.^{5,6} These interstitials are unstable with respect to the formation of chemical bonds with regular halogen ions, X^- , which leads to the X_2^- quasi molecules (called H centers) centered on halogen lattice sites. The properties of H centers are well established by means of optical, thermally activated spectroscopies, and magnetic resonance methods.⁵ Their diffusion occurs via X_2^- bond breaking and the resultant X^0 atom motion along the (110) axis through the cube face centered as a saddle point.⁶ In some alkali halides, like KCl and KBr, the H centers are oriented along the (110) axis, whereas in other crystals like

NaCl they are oriented along the (111) axis. The energy required for reorientation between these two axes is typically less than 0.1 eV. Thus, in NaCl-type crystals the H axis reorientation is a precondition for its diffusion.⁶ During their production under irradiation at low temperatures, H centers remain spatially closely correlated to their complementary electron centers — F centers — which leads to the distinctive many step (kink) decay of defect concentration during annealing.⁷

In contrast, practically nothing is known about similar properties of O_i^0 atoms in MgO,^{4,8} including the mechanism and activation energy of their thermal diffusion, important for predicting the efficiency of defect aggregation. In order to shed more light on this problem, we study, in this paper, the atomic and electronic structure, as well as the mechanism and the activation energy for diffusion of the radiation-induced O_i^0 atoms in MgO.

II. METHOD OF CALCULATION

A full-potential linear-muffin-tin-orbital (FP LMTO) method has been used.⁹ It is based on the local density approximation (LDA) for treatment of exchange and correlation effects via the Hedin-Lundqvist functional.¹⁰ This technique has been used recently¹¹ for the calculation of Fe impurities in MgO. Other *ab initio* methods recently used for MgO calculations were either based on plane waves combined with pseudopotentials,¹² or the Hartree-Fock linear combination of atomic orbitals (LCAO) method.¹³ The basic setup of our FP LMTO calculations is similar to that described in Ref. 11; O $2s$ states were included in the valence band panel and no empty spheres were used. The optimized lattice constant for pure MgO was 2.8% smaller than the experimental value of 4.21 Å, whereas the relevant bulk

modulus of $B = 15.8$ GPa was very close to the experimental data. All defect calculations were performed for the experimental lattice constant. The electronic density maps demonstrate that pure MgO is a highly ionic material, which agrees well with both previous plane-wave¹² and Hartree-Fock calculations.¹³ This allows us to treat MgO as consisting of double-charged ions Mg^{2+} and O^{2-} .

For defect calculations, the 16-atom supercell (a primitive fcc unit cell extended twice along all three translation vectors) was used, and an additional neutral O atom was added. The size of the supercell is limited by the computational time required for larger-scale calculations. This supercell allows us to optimize displacements of nearest-neighbor (NN) atoms surrounding the defect. The supercell was divided into nonoverlapping muffin-tin spheres. For an accurate comparison of total energies of any two different O_i configurations, consistent sphere radii were used. These radii were chosen as large as possible for that particular configuration pair without making further compromise with other configurations.

III. RESULTS

A. Defect geometry and energetics

We have studied four different atomic configurations (geometries) of the interstitial oxygen atom, O_i , well known in the case of H centers and shown in Fig. 1: cube centered (cc), face centered (fc), and two dumbbells [the (111) and (110) split interstitials]. Table I gives the optimized geometry (NN ion positions after relaxation) of O_i for these cases, as well as relative energies of four configurations, ΔE , and the relevant lattice relaxation energies, E_{rel} . ΔE are the relative total energies for different relaxed ionic configurations, where the (111) dumbbell configuration energy is taken as a reference energy. The relaxation energies are the differences in total energy for a perfect lattice configuration and the relaxed one. Note that for dumbbells, the starting point energy in E_{rel} calculations corresponds to the preliminary optimized distance between dumbbell atoms keeping other atoms fixed in a perfect lattice configuration. As in the previous study of a bare O vacancy in MgO,¹² we found relaxation energies very substantial.

The cc configuration is found to be energetically the *less* favorable of all four cases, even after incorporating a considerable energy gain of 3.14 eV due to NN relaxation. The unrelaxed fc configuration lies only 0.31 eV above that for unrelaxed cc. However, after a strong relaxation of four surrounding ions (5.21 eV), it turns out to be considerably more stable than the cc one. Relative displacements of the NN O(Mg) ions are (in units of the perfect Mg-O distance) 11.4% and 3.12% for cc and 12.2%, 11.2% for fc, respectively. In the former case, ionic relaxation is caused mainly by Coulomb interactions of ions, whereas in the fc case ions are compressed so densely that short-range forces start to dominate. This gives an explanation to the great asymmetry in O and Mg displacements observed in these two cases. Due to the smallness of the supercell used, we did not include relaxations of next-NN ions.

When an interstitial atom forms a dumbbell [Fig. 1(c)], it fits the crystalline lattice much better. Relevant relaxation energies for (111) and (110) dumbbells are 0.46 eV and 1.10 eV, respectively. The optimized equilibrium distances be-

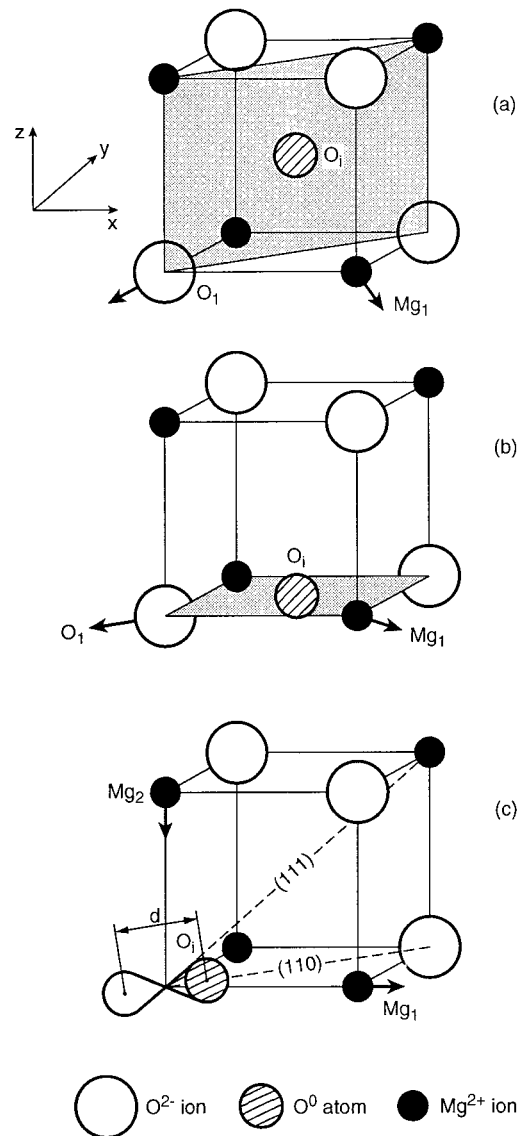


FIG. 1. Schematic sketch of possible configurations of the interstitial oxygen atom in MgO: cube centered (a), face centered (b), and the (110)-oriented dumbbell (c). Magnitudes of the atomic displacements of numbered atoms are given in Table I.

tween the two O atoms constituting the (111) and (110) dumbbells were $d = 1.36$ Å and $d = 1.38$ Å, respectively. Both dumbbell configurations lie much lower in energy than cc and fc configurations. The (111) configuration is by 0.15 eV lower in energy than the (110) one. In the case of the (110) dumbbell, two kinds of NN Mg^{2+} ions, marked as Mg_1 and Mg_2 in Fig. 1(c), have opposite directions of displacements (Table I) whereas in the case of the (111) dumbbell, they are equivalent and relax outwards relative to the dumbbell.

B. Electron density maps

Division of the supercell space as it is done in our LMTO calculations prevents us from an unambiguous analysis of effective charges on atoms, as it is usually done in HF-LCAO calculations.¹³ However, the qualitative analysis of the electronic density redistribution, due to a defect, could be performed using electron density maps.

TABLE I. Equilibrium atomic configurations of the interstitial O atom calculated for the four positions: cube centered (I), face centered (II), (111) dumbbell (III), and (110) dumbbell (IV), shown in Figs. 1(a) to (c), respectively (in units of the lattice constant a_0). Coordinates of only one atom from a set of equivalent atoms are given.

	Atomic coordinates			ΔE (eV)	E_{rel} (eV)
(I)					
O_i	0.0	0.0	0.0		
O_1	-0.283	-0.283	-0.283		
Mg_1	0.259	-0.259	-0.259	3.57	3.14
(II)					
O_i	0.0	0.0	0.0		
O_1	-0.293	-0.293	0.0		
Mg_1	0.289	-0.289	0.0	1.45	5.21
(III)					
O_i	0.094	0.094	0.094		
Mg_1	0.518	0.005	0.005	0.0	0.46
(IV)					
O_i	0.116	0.116	0.0		
Mg_1	0.532	0.003	0.0		
Mg_2	0.0	0.0	0.464	0.15	1.10

Figures 2–5 present differences between self-consistent electronic density distributions and the superposition of atomic densities for the same relaxed defect geometry, for the four O_i configurations just discussed. Thus, Fig. 2 shows the cc interstitial surrounded by four Mg and four O ions. It is obvious that the two slightly perturbed O ions at the top of

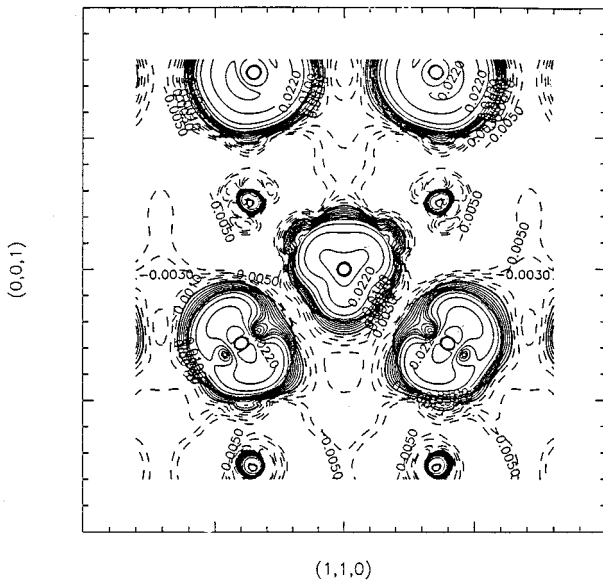


FIG. 2. Differential density map for the O_i in the cc position. Small ions are Mg, large ions are O, and the interstitial is at the center. The full and dashed lines correspond to the positive and negative charge density differences, respectively. The cross section is shown by the shaded area in Fig. 1(a). Along with five ions on this plane, one can see two other couples of O^{2-} and Mg^{2+} ions lying above and below this area.

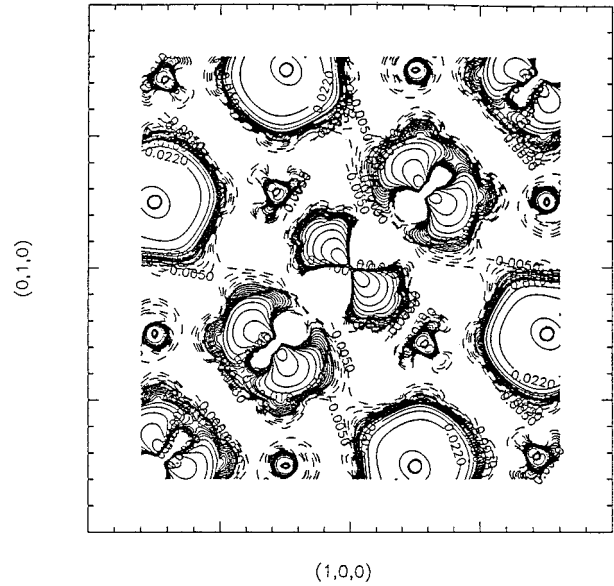


FIG. 3. Differential electronic density map for the fc configuration. The cross section is shown in Fig. 1(b). See comments to Fig. 2.

this panel are more negatively charged than the other two O ions, which are O_i NN's (the relative distances are $a_0\sqrt{11}/4$ and $a_0\sqrt{3}/4$, respectively, a_0 being the lattice constant). The interstitial oxygen demonstrates a considerable amount of electron density attracted from its four NN O^{2-} ions. The electronic density on the O_i atom is nearly the same as on each of these four ions. If we assume roughly that their totally eight (2×4) outermost electrons are equally shared by five O ions, we arrive at an effective charge of $O_i \approx -1.5e$. This means that the interstitial oxygen at cc configuration is in between O^- and O^{2-} rather a neutral atom.

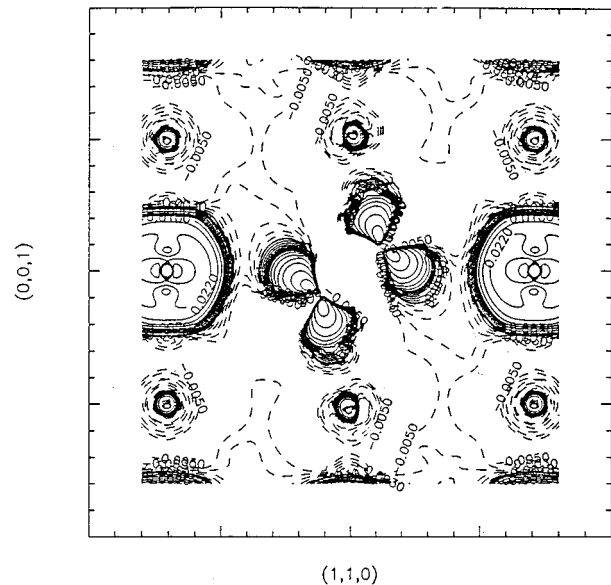


FIG. 4. Differential electronic density map for the (111) dumbbell configuration. The cross section is shown in Fig. 1(a). See comments to Fig. 2.

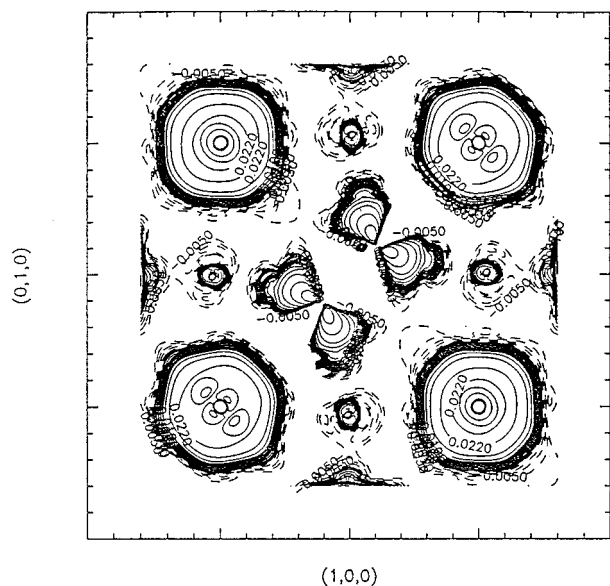


FIG. 5. Differential electronic density map for the (110) dumbbell configuration. The cross section is shown in Fig. 1(b). See comments to Fig. 2.

It should be stressed here that the electronic density distribution is sensitive to lattice relaxation.

The fc electronic density distribution is highly anisotropic (Fig. 3) and resembles a bow tie. Obviously, this is due to Coulomb repulsion of the additional electron density accumulated on O_i from the two NN O^{2-} ions. Qualitatively speaking, the electronic density on the O_i is half of that on the two NN O ions from which we can estimate the effective charge of the interstitial atom to be $\approx -1e$. In fact, it is smaller since the two NN O ions have less electron density than four only slightly perturbed next-NN O ions seen in Fig. 3.

Figures 4 and 5 demonstrate the differential maps for the two kinds of dumbbells oriented along the (111) and (110) axes. In both cases *each* of the two dumbbell atoms resembles a distorted bow tie. Unlike previous cc and fc cases discussed above, now O ions surrounding O_i are almost spherical and slightly perturbed only. This is in accord with the small relaxation energies found above for these two configurations. Since the two outermost electrons of a regular O^{2-} ion, which forms a dumbbell with an oncoming O_i^0 atom, are shared equally between these now equivalent O ions, one concludes that the effective charge of each of the two atoms is $\approx -1e$, so that the net charge on a dumbbell is close to $-2e$.

C. Diffusion mechanism

As follows from the energies of four configurations discussed above (Table I), the most favorable ground state O_i^0 configuration corresponds to the (111)-oriented dumbbell. For this configuration, the lattice distortion caused by O_i Frenkel defects is very small, in agreement with experimental data for irradiated MgO.⁸ One can imagine a 3D diffusion of oxygen interstitial atoms as a result of dumbbell breaking and subsequent O^- ion hops along the (110) axis, very simi-

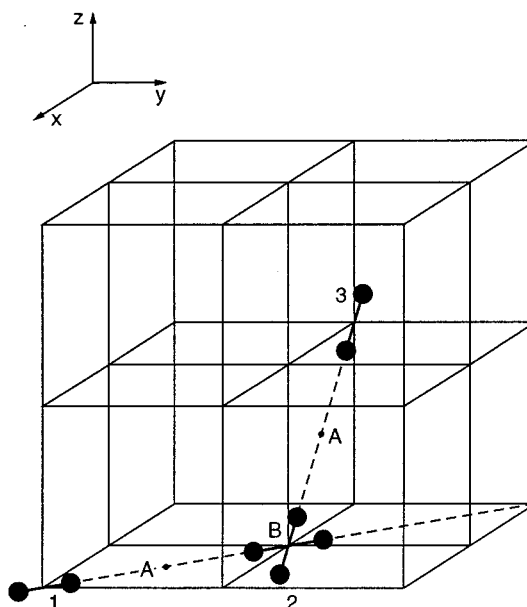


FIG. 6. The proposed mechanism (diffusion path) of the interstitial-oxygen-atom motion in MgO. See text for explanations.

lar to the behavior of the H centers in alkali halides, see Fig. 6 (positions 1-2-3). The equilibrium distance between the two atoms of a dumbbell is close to that observed for a free O_2^- molecule (1.35 Å). However, unlike both free O_2^- molecules and H centers, now there is essentially no chemical bonding between the two dumbbell atoms. Only a weak bonding is present due to the electrons in the potential well at the center, and the dumbbell atoms are mainly kept together by a balance of lattice distortion and Coulomb interaction with the surrounding ions.

The activation energy for the (110) hop (its saddle-point configuration is shown in Fig. 6, A) is 1.45 eV. It is interesting to note that a very similar magnitude of the activation energy (1.6 eV) was reported for diffusion-controlled recombination of O-related defects during their annealing in irradiated MgO samples.⁸ A dumbbell rotates easily on a lattice site, which permits it to change the lowest in energy (111) orientation for the (110) one necessary for a hop, as well as to reorient between (110) and (011) or any other equivalent orientation, with the (111) dumbbell in its saddle point (Fig. 6, B). This requires 0.15 eV of the activation energy only and does not affect the final activation energy of the diffusion controlled by the (110) hops. The hop to the cube centered position is energetically very costly and is avoided by the O_i atom.

It should be stressed here that the proposed mechanism qualitatively differs from that for the double-charge O_i^{2-} ion diffusion.¹⁴ In that case, energetically the most favorable equilibrium position is the cube centered from where ion can hop either directly along the (100) axis with the activation energy of 1.17 eV (the fc saddle point) or with lower energy via the so-called collinear interstitial mechanism characterized by a much smaller activation energy of 0.54 eV [the (111) dumbbell is the saddle point]. Such a discrepancy in the behavior of interstitial oxygen atoms depending on their

effective charge arises entirely due to quite different Coulomb interactions with surrounding ions. This point will be discussed in detail elsewhere.

D. Conclusion

The main conclusion of our study is that even if irradiation creates *neutral* interstitial oxygen atoms in MgO, they turn out to be chemically very active and transform immediately into negatively charged ions close to O_i^- , on the account of neighboring O^{2-} ions. The configuration of lowest energy corresponds to a dumbbell centered on a regular O site. The O_i diffusion is expected to be characterized by an activation energy of 1.45 eV necessary for dumbbell hops

along the (110) axis. 3D migration is achieved due to periodic rotation of the dumbbell on the lattice site, which needs much less energy (0.15 eV).

ACKNOWLEDGMENTS

The authors thank P. Ehrhart, A. Harker, P. W. M. Jacobs, A. I. Popov, V. Puchin, A. L. Shluger, and A. M. Stoneham for stimulating discussions. This study was supported by a HCM grant (T.B.) (Contract No. ERB4001GT931527), the Danish Research Council (Project No. 11-0530-1), and the EC HCM network on the Solid State Atomic Scale Simulations (Contract No. CHRX-CT93-0134) (E.K.)

-
- ¹S. J. Zinkle, Nucl. Instrum. Methods Phys. Res. B **91**, 234 (1994).
²J. Valbis and N. Itoh, Radiat. Eff. Defect Solids **116**, 171 (1991); F. W. Clinard and L. W. Hobbs, in *Physics of Radiation Effects in Crystals*, edited by R. S. Johnson and A. N. Orlov (North-Holland, Amsterdam 1986), p. 387; J. H. Crawford, Jr., Nucl. Instrum. Methods Phys. Res. Sect. B **1**, 159 (1984).
³C. Kinoshita, H. Abe, K. Fukumoto, K. Nakai, and K. Shinohara, Ultramicroscopy **39**, 205 (1991); C. Kinoshita, Y. Isobe, H. Abe, Y. Denda, and T. Sonoda, J. Nucl. Mater. **206**, 341 (1993); Y. Satoh, C. Kinoshita, and K. Nakai, *ibid.* **179-181**, 399 (1991); C. Kinoshita, K. Hayashi, and T. E. Mitchell, in *Advances in Ceramics*, edited by W. D. Kingery (American Ceramics Society, Columbus, OH, 1983), Vol. 10, p. 490.
⁴*Defects in Insulating Crystals*, edited by O. Kanert and J.-M. Spaeth (World Scientific, Singapore, 1993); Y. Chen, R. Gonzalez, V. M. Orera, and G. J. Pogatschnick, in *Disordered Systems and New Materials*, edited by M. Borissov, M. Kirov, and A. Vavrek (World Scientific, Singapore, 1989), p. 96.
⁵K. S. Song and R. T. Williams, *Self-Trapped Excitons*, Springer Series in Solid State Sciences Vol. 60 (Springer, Berlin, 1993); J.-M. Spaeth, J. R. Niklas, and R. H. Bartram, *Structural Analysis of Point Defects in Solids*, Springer Series in Solid State Sciences Vol. 43 (Springer, Berlin, 1993).
⁶E. A. Kotomin, V. E. Puchin, and P. W. M. Jacobs, Philos. Mag. **68**, 1359 (1993).
⁷E. A. Kotomin, A. I. Popov, and M. Hirai, J. Phys. Soc. Jpn. **63**, 2602 (1994).
⁸C. Scholz and P. Ehrhart, in *Beam-Solid Interactions: Fundamentals and Applications*, edited by M. A. Nastasi, L. R. Harriott, N. Herbots, and R. S. Averback, MRS Symposia Proceedings No. 279 (Materials Research Society, Pittsburgh, 1993), p. 427.
⁹M. Methfessel, Phys. Rev. B **38**, 1537 (1988); M. Methfessel, C. O. Rodriguez, and O. K. Andersen, *ibid.* **40**, 2009 (1989).
¹⁰L. Hedin and B. I. Lundqvist, J. Phys. C **4**, 2064 (1971).
¹¹M. A. Korotin, A. V. Postnikov, T. Neumann, G. Borstel, V. I. Anisimov, and M. M. Methfessel, Phys. Rev. B **49**, 6548 (1994).
¹²A. De Vita, M. J. Gillan, J. S. Lin, M. C. Payne, I. Stich, and L. J. Clarke, Phys. Rev. B **46**, 12 964 (1992).
¹³M. Causá, R. Dovesi, C. Pisani, and C. Roetti, Phys. Rev. B **33**, 1308 (1990).
¹⁴P. W. M. Jacobs and E. A. Kotomin, in *Abstracts of the International Conference on Radiation Effects in Insulators, Catania, Italy, 1995*, edited by G. Foti and O. Puglisi (Litostampa Indonea, Catania, 1995).